A New Diversity Maintenance Strategy based on the Double Granularity Grid for Multiobjective Optimization

Junzhong Ji, Yannan Weng and Cuicui Yang
College of Computer, Beijing University of Technology, Beijing Municipal Key Laboratory of Multimedia and Intelligent Software, Beijing Artificial Intelligence Institute, Pingleyuan 100, Chaoyang District, Beijing, China

Keywords: Multiobjective Optimization, Diversity Maintenance, Double Granularity Grid.

Abstract: The diversity maintenance of nondominated solutions is crucial for solving multiobjective optimization problems. The grid strategy is a very effective way to maintain the diversity of nodominated solutions, but the existing grid strategies all adopt single-layer grid structure, which has weak ability for judging the distribution of nodominated solutions in the hyperboxes with the same crowding degree. To further explore the ability of the grid strategy for maintaining the diversity of nondominated solutions, this paper presents a new diversity maintenance strategy based on the double granularity grid. The double granularity grid strategy firstly partitions the hyperboxes with the same largest crowding degree into fine granularity hyperboxes. Then, it selects nondominated individual solutions according to the solution distribution in both coarse and fine granularity hyperboxes, which can avoids randomness for selecting individual solutions in the single grid structure. To validate the performance of the double granularity grid strategy, we first integrated it with two famous algorithms, then tested the two integration algorithms by comparing them with the original algorithms and four other state-of-the-art algorithms.The experimental results validate the powerful advantages of the proposed double granularity grid strategy.

1 INTRODUCTION

Multiobjective optimization problems (MOPs) consist of multiple conflicting objectives that need to be optimized simultaneously, and widely exist in social life and engineering applications (Deb, 2001; Deb, 2014). Generally, there is no single solution for MOPs, but rather a set of alternative solutions, called Pareto optimal solutions or nondominated solutions. Population evolution-based algorithms including evolutionary and swarm intelligence algorithms, which are considered to be very suitable for solving MOPs due to their property of achieving an approximation of the Pareto in a single run (Aimin Zhou and Zhang, 2011; Margarita and Coello, 2006), and such algorithms are called evolutionary multiobjective optimization (EMO) algorithms. Over the past few decades, some well-known EMO algorithms have been proposed, such as NSGA-II (K. Deb and Meyarivan, 2000), IBEA (Eckart and Künzli, 2004), PESA-II (Corne D W, 2001), MOEA/D (Zhang and Li, 2007), MOPSO (Coello et al., 2004), NSLS (Bili Chen and Zhang, 2015) and so on. Usually, these algorithms pursue two goals: minimizing the distance between the obtained Pareto front and true the Pareto front (ie., convergence) and maximizing the distribution of the obtained Pareto optimal solutions (ie., diversity) (Ge et al., 2019). That is, most EMO algorithms need to balance both convergence and diversity in order to get a set of uniformly distributed optimal solutions. Clearly, it is very important to keep the diversity of nondominated solutions found in the optimization. Up to now, researchers have proposed different diversity maintenance strategies, including niche, clustering, *k*th nearest distance and grid (Li et al., 2014).

In the existing diversity maintenance strategies, the grid strategy has an inherent property of reflecting the diversity of individuals in a population (Yang et al., 2013; X. Cai and Zhang, 2017). Corne and Knowles developed PAES algorithm (Pareto Archive Evolution Strategy) (JD and DW, 2000), which is the first algorithm to introduce the grid strategy to maintain the diversity of the nondominated solutions. Afterwards, they proposed other two different algorithms, PESA (The Pareto Envelope-based selection algorithm) (Corne et al., 2000) and PESA-II (Corne D W, 2001), based on the grid strategy. PESA adopts individual selection based on the grid strategy, and PESA-II uses region selection. Coello et al. pre-

Ji, J., Weng, Y. and Yang, C.
A New Diversity Maintenance Strategy based on the Double Granularity Grid for Multiobjective Optimization.
DOI: 10.5220/0009167500880095
In *Proceedings of the 9th International Conference on Pattern Recognition Applications and Methods (ICPRAM 2020)*, pages 88-95
ISBN: 978-989-758-397-1; ISSN: 2184-4313

sented MOPSO algorithm (Handling Multiple Objectives With Particle Swarm Optimization) (Coello et al., 2004), which adopted the adaptive grid strategy to preserve the diversity of nondominated solutions. These existing grid-based algorithms have proved the validity of the grid strategy in maintaining the diversity of nondominated solutions. However, these algorithms only use single-layer grid structure, and randomly select a hyperbox or an individual when multiple hyperboxes contain the same amount of individuals, which may undermine the diversity of the nondominated solutions in the crowded area.

To further explore the ability of the grid strategy for maintaining the diversity of nondominated solutions, this paper presents a novel diversity maintenance strategy based on the double granularity grid(DGG) strategy. The DGG strategy partitions the hyperboxes with the same largest crowding degree into fine granularity hyperboxes to more precisely locate the position of the nondominated solutions, which can avoid randomness for selecting hyperboxes and individual solutions in the single grid structure.

To verify the effectiveness of DGG strategy, we first integrated it into two algorithms based on the single-layer grid structure to generate two new integration algorithms. Then tested the two new integrated algorithms by comparing them with the original algorithm and four other EMO algorithms.

The rest of this paper is organized as follows. Section 2 briefly introduces basic concepts involving MOPs. Section 3 is devoted to describing the details of the proposed method. Next, Section 4 presents the experimental design and results. Section 5 concludes this paper and outlines future research directions.

2 BASIC CONCEPTS

Without loss of generality, a MOP may be stated as a minimization problem and defined as follows (Deb, 2001):

$$\begin{cases} min & y = F(\mathbf{x}) = (f_1(\mathbf{x}), f_2(\mathbf{x}), \cdots, f_m(\mathbf{x}))^T \\ s.t. & g_i(\mathbf{x}) \leq 0, i = 1,2,\cdots,p \\ & h_j(\mathbf{x}) = 0, j = 1,2,\cdots,q \\ & x_i^L \leq x_i \leq x_i^U \end{cases} \tag{1}$$

where $\mathbf{x} = (x_1, x_2, \cdots, x_n) \in X \subset R^n$ is a n-dimensional decision vector, X represents a n-dimensional decision space, x_i^L and x_i^U are the upper and lower boundary values of x_i, respectively. $y = (y_1, y_2, \cdots, x_m) \in Y \subset R^m$ is a m-dimensional objective vector, Y represents a m-dimensional objective space. $F(\mathbf{x})$ is a mapping function from n-dimensional decision space to m-dimensional objective space. $g_i(\mathbf{x}) \leq 0$ $(i = 1,2,\cdots,p)$ and $h_j(\mathbf{x}) = 0$ $(j = 1,2,\cdots,q)$ defines p inequalities and q equalities, respectively.

In the following, we will list four definitions involving MOPs.

Definition 1 (Pareto Dominant). $\mathbf{x}^\alpha$, $\mathbf{x}^\beta$ are two feasible solutions, $\mathbf{x}^\alpha$ is Pareto dominant compared with $\mathbf{x}^\beta$ if and only if:

$$\begin{array}{l} \forall i = 1,2,\cdots,m, f_i(\mathbf{x}^\alpha) \leq f_i(\mathbf{x}^\beta) \wedge \\ \exists j = 1,2,\cdots,m, f_i(\mathbf{x}^\alpha) < f_i(\mathbf{x}^\beta) \end{array}. \tag{2}$$

We call this relationship $\mathbf{x}^\alpha \succ \mathbf{x}^\beta$, $\mathbf{x}^\alpha$ dominate $\mathbf{x}^\beta$, or $\mathbf{x}^\beta$ is dominated by $\mathbf{x}^\alpha$.

Definition 2 (Pareto Optimal Solution). Ω is the feasible solution set, $\mathbf{x}^* \in \Omega$, $\mathbf{x}^*$ is a Pareto optimal solution if and only if:

$$\neg\exists \mathbf{x} \in \Omega : \mathbf{x} \succ \mathbf{x}^*. \tag{3}$$

Definition 3 (Pareto Optimal Set). The Pareto optimal set includes all the Pareto optimal solutions and is given as follows:

$$X^* = \{\mathbf{x}^* | \neg\exists \mathbf{x} \in \Omega : \mathbf{x} \succ \mathbf{x}^*\}. \tag{4}$$

Definition 4 (Pareto Front). The Pareto front (noted as **PF**) includes all the objective vectors corresponding to X^* and is given as follows:

$$PF = \{F(\mathbf{x}^*) = (f_1(\mathbf{x}^*), f_2(\mathbf{x}^*), \cdots, f_m(\mathbf{x}^*))^T | \mathbf{x}^* \in X^*\}. \tag{5}$$

For better distinction, we present the true **PF** and the **PF** obtained by an algorithm as $\mathbf{PF}_{true}$ and PF_{approx} respectively.

3 DOUBLE GRANULARITY GRID (DGG) STRATEGY

Usually, the EMO algorithms set in two populations: an internal population and an external population (also called archive set (**EA**)). The internal population executes optimization mechanisms, and the external population preserves the nondominated solutions obtained in the optimization process. When the size of **EA** exceeds the specified quantity, the DGG strategy is used to remove redundant solutions and maintain the diversity of nondominated solutions. As shown in the **Strategy 1**, implementation of this strategy includes the following two steps.

Step 1) Coarse Granularity Grid Partition. The objective space region is divided into coarse granularity that **EA** occupies into hyperboxes, and $div1$ represents the number of first partition for each dimensional objective space. At the same time, some relevante information, including the lower and upper boundaries of the grid, the width and grid coordinate

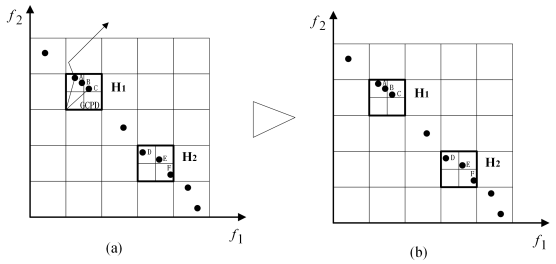

Figure 1: Schematic diagram of the double granularity grid strategy.

Strategy 1: Double Granularity Grid Strategy.

1 **while EA exceeding specified quantity**
2 **Make a coarse granularity partition** on the objective space region that **EA** occupy.
3 i) If only one coarse hyperbox has the highest crowding degree (denoted by δ)
4 • Compute the *GCPD* of each individual in this coarse hyperbox as Eq.(10);
5 • Remove the individual with the largest value of *GCPD*.
6 ii) If more than one coarse hyperbox have the same δ
7 • **Make a fine granularity partition** on the coarse hyperboxes;
8 • Calculate the E of these coarse hyperboxes based on the δ of fine hyperboxes as Eq.(11);
9 • Select the coarse hyperbox with the smallest value of E;
10 • Remove the individual with the largest value of *GCPD* in the selected coarse hyperbox.
11 **end while**

of each dimensional objective for each coarse granularity hyperbox, is provided. Each individual solution in **EA** has an exact position in a coarse granularity hyperbox. Each coarse granularity hyperbox has a crowding degree attribute denoted by δ, which represents the total number of individual solutions contained in this coarse granularity hyperbox. In addition, each coarse granularity hyperbox has a m-dimensional grid coordinate, and its kth grid coordinate is defined as follows.

For the kth objective, the lower and upper boundaries of the grid are determined according to the following formula:

$$lb_k = min_k(\mathbf{EA}) - (max_k(\mathbf{EA}) - min_k(\mathbf{EA}))/(2 * div1) \quad (6)$$

$$ub_k = max_k(\mathbf{EA}) + (max_k(\mathbf{EA}) - min_k(\mathbf{EA}))/(2 * div1) \quad (7)$$

where $max_k(\mathbf{EA})$ and $min_k(\mathbf{EA})$ stand for the minimal and maximal values in the kth objective, respectively.

The coarse granularity hyperbox width in the kth objective can be formed as:

$$d_k = (ub_k - lb_k)/div1 \quad (8)$$

The grid coordinates of an individual on the kth objective is defined as:

$$G_k(\mathbf{x}) = floor((f_k(\mathbf{x}) - lb_k)/d_k) \quad (9)$$

where $f_k(\mathbf{x})$ is the actual kth objective value.

Step 2) Fine Granularity Grid Partition. When the **EA** exceeds the specified size, the individual in coarse granularity hyperbox with maximum crowding degree is continuously reduced one by one until the capacity of **EA** reaches the specified number. If only one coarse granularity hyperbox has the maximum crowding degree, calculate the grid coordinate point distance (GCPD) for each individual in the hyperbox, and then select the individual with the highest GCPD value to delete. Here *GCPD* is a useful criteria to discriminate individuals in the same hyberbox, and is defined as (Yang et al., 2013):

$$GCPD(\mathbf{x}) = \sqrt{\sum_{k=1}^{m} ((f_k(\mathbf{x}) - (lb_k + G_k(\mathbf{x}) * d_k))/d_k)^2} \quad (10)$$

where m is the number of objectives.

There is another situation where multiple coarse granularity hyperboxes have the same maximum crowding degree. In this case, first divide those coarse granularity hyperboxes further with partition number $div2$ and calculate the crowding degree of each fine granularity hyperbox. Then, according to the crowding degree of fine granularity hyperboxes, calculate the evenness index of the corresponding coarse granularity hyperbox and choose the coarse granularity hyperbox with the smallest evenness index. At last, compute the GCPD value of all the individual solutions in the selected coarse granularity hyperbox and remove the one with largest value of GDPD. The evenness index is diffusely used to measure the evenness of individual solutions distribution in a population and is defined as (E. Elejalde and Bollen, 2018):

$$E = \frac{-\sum_{i=1}^{C} \frac{n_i}{N} * ln\frac{n_i}{N}}{lnC} \quad (11)$$

where C is the number of fine granularity hyperboxes in the coarse granularity hyperbox, and $C = (div2)^m$, N is the crowding degree of the coarse granularity hyperbox, n_i is the crowding degree of the fine granularity hyperbox i.

From the above can be obtained, compared with the single-layer grid structure, the proposed DGG

Table 1: Comparison results of PESA-II and PESA-II+DGG on the UF suit.

Problems	*IGD*		*HV*	
	PESA-II	PESA-II+DGG	PESA-II	PESA-II+DGG
UF1	1.6746E−1(5.26E−2)	**1.5827E−1(4.77E−2)**	5.3944E−1(4.43E−2)	**5.5198E−1(4.77E−2)**
UF2	8.1915E−2(2.28E−2)	**7.5380E−2(2.44E−2)**	6.3582E−1(1.35E−2)	**6.3947E−1(1.69E−2)**
UF3	3.0906E−1(3.65E−2)	**3.0581E−1(3.72E−2)**	3.9149E−1(4.26E−2)	**3.9866E−1(3.00E−2)**
UF4	5.4234E−2(2.42E−3)	**5.3642E−2(1.29E−3)**	3.6967E−1(3.89E−3)	**3.6973E−1(2.41E−3)**
UF5	9.3133E−1(2.42E−1)	**8.6005E−1(2.01E−1)**	4.1482E−3(1.25E−2)	**4.8915E−3(1.20E−2)**
UF6	3.4004E−1(1.30E−1)	**3.2328E−1(1.26E−1)**	2.3587E−1(6.43E−2)	**2.4043E−1(6.96E−2)**
UF7	3.1960E−1(1.52E−1)	**2.9626E−1(1.93E−1)**	3.2372E−1(9.32E−2)	**3.4040E−1(1.19E−1)**

Table 2: Comparison results of PESA-II and PESA-II+DGG on the DTLZ suit.

Problems	*IGD*		*HV*	
	PESA-II	PESA-II+DGG	PESA-II	PESA-II+DGG
DTLZ1	2.8645E−2(5.00E−2)	**1.9636E−2(1.59E−2)**	8.0912E−1(1.17E−1)	**8.2774E−1(7.97E−3)**
DTLZ2	5.7137E−2(7.95E−3)	**5.6004E−2(6.27E−3)**	5.4325E−1(7.99E−3)	**5.4030E−1(7.32E−3)**
DTLZ3	1.4474E+0(1.41E+0)	**1.3363E+0(1.20E+0)**	1.5604E−1(2.28E−1)	**1.5676E−1(2.40E−1)**
DTLZ4	5.4250E−2(3.53E−3)	**5.2816E−2(3.13E−3)**	5.4765E−1(8.46E−3)	**5.4795E−1(6.81E−3)**
DTLZ5	4.4671E−3(3.92E−4)	**4.3857E−3(2.79E−4)**	1.9874E−1(2.06E−3)	**1.9916E−1(9.33E−4)**
DTLZ6	5.0470E−3(3.08E−4)	**4.9680E−3(2.52E−4)**	1.9827E−1(2.05E−3)	**1.9831E−1(1.98E−3)**
DTLZ7	5.4475E−2(5.61E−2)	**4.4917E−2(1.74E−3)**	2.7794E−1(7.08E−3)	**2.7853E−1(2.78E−3)**

strategy has two differences. On the one hand, when there are multiple coarse granularity hyperboxes with largest crowding degree, they are further divided into fine granularity hyperboxes. On the other hand, GCPD is used as the basis for individual selection. Therefore, the DGG strategy enhances the resolution of the hyperbox, avoids the randomness of the hyperbox and solution selection, and enables the distribution of nondominated solutions more uniform.

For clarity, Fig.1 shows a simple two-dimensional example. Fig.1 (a) gives an **EA** that holds all nondominated solutions, the number of solutions which exceed the maximum capacity of the **EA** is 1. Thus, the DGG strategy is used to eliminate one redundant solution. Firstly, divide the objective space of the **EA** to get coarse granularity hyperboxes with the partition number of 5, and find the coarse granularity hyperbox with the largest crowding degree. As shown in Fig.1 (a), $\mathbf{H}_1$ and $\mathbf{H}_2$ are the two coarse granularity hyperboxes with biggest crowding degree, which consists of three individuals. Secondly, a fine granularity partition in $\mathbf{H}_1$ and $\mathbf{H}_2$ for fine granularity hyperbox, the number of partitions is 2 and calculate the evenness of $\mathbf{H}_1$ and $\mathbf{H}_2$, select the $\mathbf{H}_1$ with smaller evenness according to Eq.(10). Finally, compute the GCDP of individual **A**, **B** and **C** in the coarse granularity hyperbox $\mathbf{H}_1$ according to Eq.(11), choose the individual **A** with the largest value and remove it from the **EA**, and obtain the final nondominated solution set as shown in Fig.1(b).

4 EXPERIMENTS

In this section, extensive experiments have verified the performance of the proposed DGG strategy. The experimental platform is a PC with Intel(R) Core(TM) i5-4590 CPU 3.30GHz, 8GB RAM, and Windows 10, and DGG is implemented using the Matlab language.

4.1 Experimental Setting

Two well-defined test suites, the UF (Huband et al., 2005) and DTLZ (K. Deb and Zitzler, 2005), are selected in this paper. UF1-UF7 are bi-objective test problems, and DTLZ1-DTLZ7 are tri-objective test problems to further examine the performance of the DGG strategy in handling MOPs with more than two objectives. We chose two evaluation metrics: the inverted generational distance(IGD) (Bosman and Thierens, 2003) and hypervolume (HV) (Z. Eckart and Lothar, 2008), which can check convergence and diversity simultaneously.

Let S^* be a set of uniformly distributed solutions along $\mathbf{PF}_{true}$ and S be the set of obtained solutions along $\mathbf{PF}_{approx}$. *IGD* measures the average distance from S^* to S and is defined as follows:

$$IGD(S,S^*) = \frac{1}{|S^*|}\sum_{\mathbf{x}^*\in S^*} d(\mathbf{x}^*,S) \tag{12}$$

where $d(\mathbf{x}^*,S)$ is the Euclidean distance between the solution $\mathbf{x}^*$ and its nearest point in S, and $|S^*|$ is

Table 3: Comparison results of MOPSO and MOPSO+DGG on the UF suit.

Problems	*IGD*		*HV*	
	MOPSO	MOPSO+DGG	MOPSO	MOPSO+DGG
UF1	5.8264E−1(1.19E−1)	**5.3610E−1(1.11E−1)**	1.2827E−1(6.42E−2)	**1.6000E−1(6.18E−2)**
UF2	1.0720E−1(1.15E−2)	**1.0297E−1(1.55E−2)**	5.9727E−1(1.27E−2)	**6.0335E−1(1.39E−2)**
UF3	5.3750E−1(2.50E−2)	**5.2532E−1(2.52E−2)**	1.3988E−1(2.02E−2)	**1.4386E−1(2.01E−2)**
UF4	9.3645E−2(1.05E−2)	**8.8813E−2(6.96E−3)**	3.1497E−1(1.20E−2)	**3.1747E−1(1.14E−2)**
UF5	3.3849E+0(3.17E−1)	**3.3509E+0(3.12E−1)**	0.0000E+0(0.00E+0)	0.0000E+0(0.00E+0)
UF6	2.7668E+0(4.94E−1)	**2.6966E+0(5.77E−1)**	0.0000E+0(0.00E+0)	0.0000E+0(0.00E+0)
UF7	6.6809E−1(1.11E−1)	**6.1686E−1(9.34E−2)**	3.3508E−2(3.03E−2)	**4.4364E−2(4.64E−2)**

Table 4: Comparison results of MOPSO and MOPSO+DGG on the DTLZ suit.

Problems	*IGD*		*HV*	
	MOPSO	MOPSO+DGG	MOPSO	MOPSO+DGG
DTLZ1	4.9920E+0(2.11E+0)	**3.9530E+0(1.24E+0)**	0.0000E+(0.00E+0)	0.0000E+(0.00E+0)
DTLZ2	2.0996E−1(4.25E−2)	**2.0033E−1(5.16E−2)**	3.6641E−1(2.78E−2)	**3.7842E−1(3.15E−2)**
DTLZ3	7.2673E+1(4.89E+1)	**5.9949E+1(4.38E+1)**	0.0000E+0(0.00E+0)	**1.8080E−3(9.90E−3)**
DTLZ4	2.3055E−1(1.08E−1)	**2.2383E−1(5.57E−2)**	4.5579E−1(3.74E−2)	**4.6480E−1(3.91E−2)**
DTLZ5	**4.1721E−3(4.62E−4)**	6.5022E−3(2.12E−4)	**1.9916E−1(6.34E−4)**	1.9802E−1(2.06E−4)
DTLZ6	2.6758E+0(1.44E+0)	**2.5944E+0(1.04E+0)**	1.9695E−2(6.01E−2)	**1.9809E−2(3.62E−2)**
DTLZ7	6.0958E+0(1.87E+0)	**5.7735E+0(1.54E+0)**	0.0000E+(0.00E+0)	0.0000E+(0.00E+0)

the size of the set S^*. In general, a lower value of $IGD(S,S^*)$ indicates that S more evenly covers $\mathbf{PF}_{approx}$ and is closer to $\mathbf{PF}_{true}$.

Let $\mathbf{z}^r = (z_1^r, z_2^r, \ldots, z_m^r)^T$ be a reference point in the objective space that is dominated by all Pareto optimal objective vectors. Let S be the obtained approximation set (i.e., PF_{approx}) of PF_{true} in the objective space. HV measures the volume of the region dominated by S and bounded by $\mathbf{z}^r$) and a larger value is preferable, it's defined as:

$$HV(S) = volume\left(\bigcup_{\mathbf{x}\in S}[x_1, z_1^r] \times \ldots \times [x_m, z_m^r]\right) \quad (13)$$

To verify the proposed DGG strategy, we integrate DGG strategy into two classical EMO algorithms based on the single-layer grid structure PESA-II and MOPSO, which results in two new algorithms, denoted by PESA-II+DGG and MOPSO+DGG, respectively. Firstly, we separately compare the two new algorithms with their corresponding original versions. Thereafter, we select one of the new algorithms and compare it with the other four state-of-the-art EMO algorithms to further demonstrate the effectiveness of the proposed method.

The number of coarse granularity grid division $div1$ in two new algorithms was set as 32 and 30, which was consistent with the number of grid in the original algorithm, and the quantity of fine grid division $div2$ is set as 2, the population and **EA** size were set to 100. All the results presented in this paper are obtained by executing 30 independent runs of each algorithm on each test problem with the termination criterion of 50,000 evaluations. For the other parameters in all algorithms, we tried to use identical settings as suggested in original studies.

4.2 Original Algorithm vs Original Algorithm+DGG

Table 1 and Table 2 show the comparative results of the PESA-II and PESA-II+DGG on the UF and DTLZ test suites regrading the mean and standard deviation values, with respect to the two metrics IGD and HV. The best average result with respect to each metric are show in bold. As can be seen from Table 1 and Table 2 that whether IGD metric or HV metric, PESA-II+DGG plays best on all the 14 test instances, represents a better performance than PESA-II.

The experimental results of MOPSO and MOPSO+DGG are listed in Table 3 and Table 4. As shown in Table3, MOPSO+DGG achieves best values for all UF test problems in addition to the HV metric value on UF5 and UF6, and neither algorithms converge on UF5 and UF6. About the IGD metric on the DTLZ test suite, MOPSO+DGG plays best on six out of seven test problems except the DTLZ5. Regarding HV metric, MOPSO+DGG

Table 5: Comparison results of the five algorithms on the UF and DTLZ test suites in term of *IGD*.

Problems	NSGA-II	MOED/D	IBEA	NSLS	PESA-II+DGG
UF1	1.6537E−1(5.62E−2)	2.7100E−1(1.00E−1)	1.6278E−1(4.88E−2)	2.5520E−1(2.76E−2)	**1.5827E−1(4.77E−2)**
UF2	**6.1831E−2(2.01E−2)**	1.7084E−1(8.07E−2)	6.2608E−2(1.71E−2)	5.5395E−1(3.79E−2)	7.5380E−2(2.44E−2)
UF3	2.9459E−1(4.59E−2)	3.2462E−1(2.43E−2)	**2.8530E−1(4.68E−2)**	3.8590E−1(2.52E−3)	3.0581E−1(3.72E−2)
UF4	5.4031E−2(2.52E−3)	8.3697E−2(3.74E−3)	5.8447E−2(4.15E−3)	7.0373E−2(5.45E−3)	**5.3647E−2(1.29E−3)**
UF5	7.5661E−1(1.86E−1)	**5.9337E−1(1.28E−1)**	6.4726E−1(1.75E−1)	1.9925E+0(1.23E−1)	8.6005E−1(2.01E−1)
UF6	3.3181E−1(1.33E−1)	4.7767E−1(2.41E−1)	3.5317E−1(2.18E−1)	1.0892E+0(7.78E−2)	**3.2328E−1(1.26E−1)**
UF7	2.4500E−1(1.54E−1)	4.1291E−1(1.65E−1)	**1.9426E−1(1.53E−1)**	2.7945E−1(2.31E−2)	2.9626E−1(1.93E−1)
DTLZ1	3.1601E−1(2.30E−1)	2.0636E−2(7.14E−5)	1.6766E−1(1.00E−1)	2.9003E+1(3.10E+0)	**1.9636E−2(1.59E−3)**
DTLZ2	6.9104E−2(2.03E−3)	**5.4464E−2(4.63E−7)**	8.1858E−2(2.11E−3)	4.1622E−1(5.14E−2)	5.6004E−2(6.27E−3)
DTLZ3	3.1061E+0(1.93E+0)	**5.9815E−2(4.36E−3)**	2.7884E+0(2.41E+0)	1.6674E+2(141E+1)	1.3363E+0(1.20E+0)
DTLZ4	9.8091E−2(1.60E−1)	2.1377E−1(2.57E−1)	1.0997E−1(1.58E−1)	6.0497E−1(6.17E−2)	**5.2816E−2(3.13E−3)**
DTLZ5	5.6405E−3(3.15E−4)	3.3865E−2(3.13E−5)	1.6502E−2(1.69E−3)	3.7154E−1(5.20E−2)	**4.3857E−3(2.79E−4)**
DTLZ6	6.0003E−3(2.96E−4)	3.3911E−2(8.69E−6)	1.8060E−2(2.37E−3)	2.1798E−1(8.01E−2)	**4.9680E−3(2.52E−4)**
DTLZ7	8.5549E−2(4.99E−2)	1.9806E−1(1.64E−1)	9.7567E−2(7.63E−2)	5.0053E−1(6.03E−2)	**4.4917E−2(1.74E−3)**

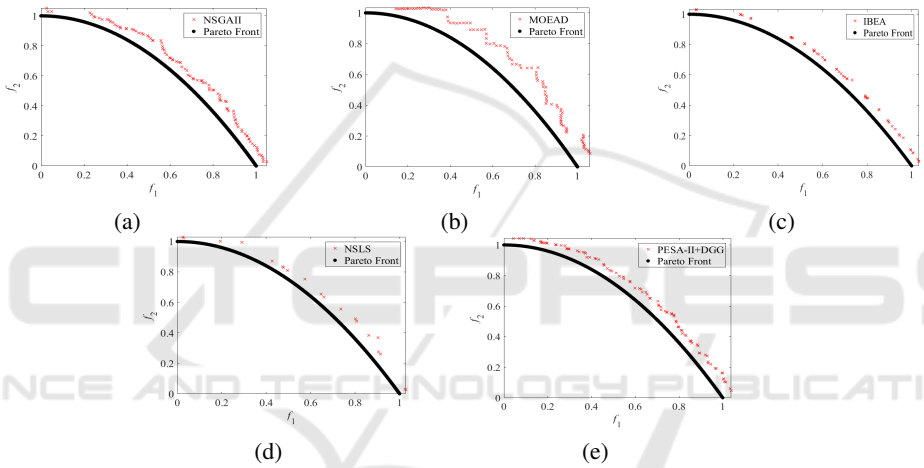

Figure 2: Approximations of $\mathbf{PF}_{true}$ found by different algorithms on UF4: (a) NSGA-II, (b) MOEA/D, (c) IBEA, (d) NSLS and (e) PESA-II+DGG.

produces the best results on four out of seven test problems: DTLZ2, DTLZ3, DTLZ4 and DTLZ6 and both MOPSO+DGG and MOPSO failed to converge effectively on DTLZ1 and DTLZ7 test problems.

4.3 Comparisons with State-of-the-Art Algorithms

To further demonstrate the performance of the proposed strategy, we choose one integration algorithm PESA-II+DGG to compare with four state-of-the-art algorithms. Tables 5 gives the results of all the algorithms on the UF and DTLZ test suites in terms of IGD metric. Regarding UF test suite, PESA-II+DGG plays best on three out of seven test problems: UF1, UF4 and UF6. IBEA attains the best results on UF3 and UF7 while NSGA-II obtains the best results on UF2 and MOEA/D achieves a better value on UF5. Concerning the DTLZ test suite, PESA-II+DGG strategy gets the best performance on all the test problems except DTLZ2 and DTLZ3, while MOEA/D yields the best results on DTLZ1 and DTLZ3.

Table 6 shows the results in terms of HV on the two test suites. About the UF test suite, PESA-II+DGG strategy produces the best results on three test problems: UF1, UF4 and UF6, with MOEA/D on UF5, and with NSGA-II performs best on UF2, UF3 and UF7. For the DTLZ test suite, PESA-II+DGG strategy performs best in three test problems including DTLZ4, DTLZ5 and DTLZ7. MOEA/D gets the best values on DTLZ1, DTLZ2 and DTLZ3, while NSGA-II obtains the best results on DTLZ6.

To intuitively illustrate the results of different algorithms, we plot their final $\mathbf{PF}_{approx}$ on UF4 and

Table 6: Comparison results of the five algorithms on the UF and DTLZ test suites in term of HV.

Problems	NSGA-II	MOEA/D	IBEA	NSLS	PESA-II+DGG
UF1	5.4521E−1(9.40E−2)	4.6001E−1(6.06E−2)	5.4568E−1(5.59E−2)	3.5544E−1(3.81E−2)	**5.5198E−1(4.77E−2)**
UF2	**7.9102E−1(1.21E−2)**	6.0930E−1(3.98E−2)	6.5537E−1(1.09E−2)	9.4796E−2(2.32E−2)	6.3947E−1(1.69E−2)
UF3	**4.0706E−1(5.76E−2)**	3.6294E−1(2.68E−2)	3.9449E−1(2.40E−2)	1.8994E−1(8.22E−3)	3.9866E−1(3.00E−2)
UF4	3.6256E−1(1.67E−2)	3.2340E−1(4.38E−3)	3.6811E−1(3.73E−3)	3.5117E−1(4.91E−3)	**3.6973E−1(2.41E−3)**
UF5	1.1454E−2(2.23E−2)	**8.1769E−2(6.80E−2)**	3.6548E−2(4.78E−2)	0.0000E+0(0.00E+0)	4.8915E−3(1.20E−2)
UF6	2.3175E−1(1.10E−1)	1.8840E−1(9.45E−2)	2.3286E−1(8.07E−2)	0.0000E+0(0.00E+0)	**2.4.43E−1(6.96E−2)**
UF7	**4.4303E−1(1.19E−1)**	2.6239E−1(1.06E−1)	4.0917E−1(1.01E−1)	1.6539E−1(3.51E−2)	3.4010E−1(1.19E−1)
DTLZ1	2.9097E−1(3.32E−1)	**8.4082E−1(7.12E−4)**	5.3077E−1(2.09E−1)	0.0000E+0(0.00E+0)	8.2774E−1(7.97E−3)
DTLZ2	5.3650E−1(3.53E−3)	**5.5960E−1(6.44E−6)**	5.5744E−1(1.19E−3)	4.6034E−2(3.80E−2)	5.4030E−1(7.32E−3)
DTLZ3	9.5069E−3(5.21E−2)	**5.3461E−1(1.37E−2)**	7.4213E−3(4.06E−2)	0.0000E+0(0.00E+0)	1.5676E−1(2.40E−1)
DTLZ4	5.2098E−1(8.15E−2)	4.8533E−1(1.23E−1)	5.4225E−1(8.53E−2)	0.0000E+0(0.00E+0)	**5.4795E−1(6.81E−3)**
DTLZ5	1.9853E−1(1.41E−4)	1.8188E−1(1.32E−5)	1.9869E−1(3.04E−4)	2.8943E−3(5.18E−3)	**1.9916E−1(9.33E−4)**
DTLZ6	**1.9935E−1(1.43E−4)**	1.8185E−1(4.19E−6)	1.9821E−1(4.39E−4)	1.2118E−1(1.77E−2)	1.9831E−1(1.98E−3)
DTLZ7	2.6915E−1(5.84E−3)	2.5216E−1(1.35E−2)	2.7431E−1(1.00E−2)	1.2069E−1(2.26E−2)	**2.7853E−1(2.78E−3)**

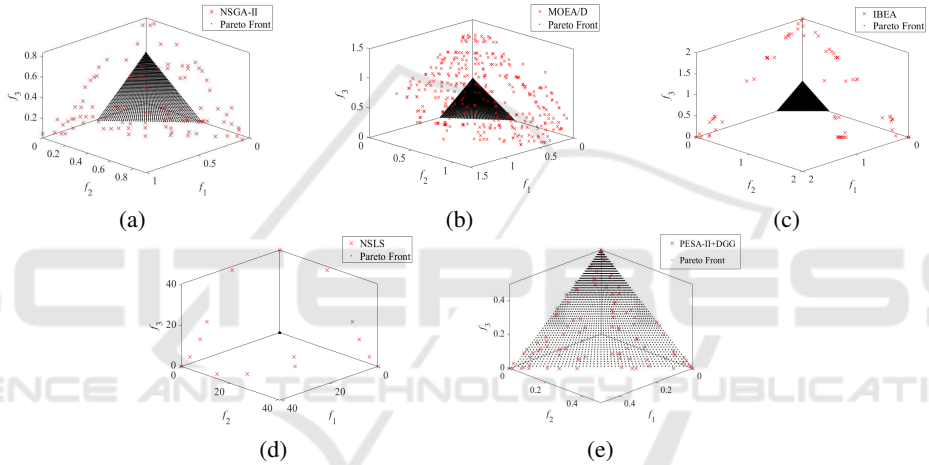

(a) (b) (c) (d) (e)

Figure 3: Approximations of $\mathbf{PF}_{true}$ found by different algorithms on UF4: (a) NSGA-II, (b) MOEA/D, (c) IBEA, (d) NSLS and (e) PESA-II+DGG.

DTLZ1 test problems, in Fig. 2 and Fig. 3, respectively. As can be seen from Fig. 2, the $\mathbf{PF}_{approx}$ of MOPSO-DGG is very close to the $\mathbf{PF}_{true}$ and the obtained nondominated solutions are uniformly distributed on $\mathbf{PF}_{approx}$, and the other four algorithms fail to cover the $\mathbf{PF}_{true}$.

5 CONCLUSIONS

The diversity of nondominated solutions is a momentous goal of evolutionary and swarm intelligence algorithms for solving MOPs. The grid strategy is an effective diversity maintenance strategy of nondominated solutions. However, the existing grid strategy based on single-layer grid structure can not judge the diversity of nondominated solutions in multiple hyperboxes with the same crowding degree. In this paper, we proposed a new diversity maintainance strategy based on the double granularity grid (DGG), which obtains the more evenly distribution of nondominated solutions by dividing double granularity grid. To demonstrate the performance of DGG strategy, we integrated it with two popular algorithms based on single-layer grid and compared it with four state-of-the-art algorithms. The experimental results show that the proposed DGG strategy is effective and has great potential for maintaining the diversity of nondominated solutions on MOPs problems.

In the future, we will further study the grid strategy and develop a more effective diversity maintenance strategy. Since the results of the proposed strategy in many-objective optimization problem are not very ideal, we also want to extend this strategy to the many-objective optimization problem in the next step.

ACKNOWLEDGEMENTS

This work is partly supported by the NSFC Research Program (61672065, 61906010), Beijing Municipal Education Research Plan Project (KM202010005032), China Postdoctoral Science Foundation funded project (71007011201801), Beijing Postdoctoral Research Foundation (2017-ZZ-024), and Chaoyang Postdoctoral Research Foundation (2018ZZ-01-05).

REFERENCES

Aimin Zhou, Bo-Yang Qu, H. L. S.-Z. Z. and Zhang, Q. (2011). Multiobjective evolutionary algorithms: A survey of the state of the art. *Swarm and Evolutionary Computation*, volume 1, pages 32–49.

Bili Chen, Wenhua Zeng, Y. L. and Zhang, D. (2015). A new local search-based multiobjective optimization algorithm. *IEEE Transactions on Evolutionary Computation*, volume 19, pages 50–73.

Bosman, P. and Thierens, D. (2003). The balance between proximity and diversity in multiobjective evolutionary algorithms. *IEEE Transactions on Evolutionary Computation*, volume 7, pages 174–188.

Coello, C. A., Pulido, G. T., and Lechuga, M. S. (2004). Handling multiple objectives with particle swarm optimization. *IEEE Transactions on Evolutionary Computation*, volume 8, pages 256–279.

Corne, D., Knowles, J., and Oates, M. (2000). The pareto-envelope based selection algorithm for multiobjective optimization. In*International Conference on Parallel Problem Solving from Nature*, pages 869–878.

Corne D W, Jerram N R, K. J. D. e. a. (2001). PESA-II: Region-based selection in evolutionary multiobjective optimization. In *GECCO'2001' Proceedings of the Genetic and Evolutionary Computation Conference*, pages 283–290.

Deb (2001). *Multi-objective Optimization using Evoulutionary Algorithms*. Chichester, john wiley & sons edition.

Deb (2014). *Multi-objective Optimization, Search methodologies*. Springer, Boston,MA.

E. Elejalde, L. Ferres, E. H. and Bollen, J. (2018). Quantifying the ecological diversity and health of online news. *Journal of computational science*, volume 27, pages 218–226.

Eckart, Z. and Künzli, S. (2004). Indicator-based selection in multiobjective search. In *in Proc. 8th International Conference on Parallel Problem Solving from Nature (PPSN VIII)*, pages 832–842. Springer.

Ge, H., Zhao, M., Sun, L., Wang, Z., Tan, G., Zhang, Q., and Chen, C. L. P. (2019). A many-objective evolutionary algorithm with two interacting processes: Cascade clustering and reference point incremental learning. *IEEE Transactions on Evolutionary Computation*, pages 1–1.

Huband, S., Barone, L., While, L., and Hingston, P. (2005). A scalable multi-objective test problem toolkit. *In Evolutionary Multiobjective Optimization*,Springer.

JD, K. and DW, C. (2000). Approximating the non-dominated front using the pareto archived evoluton strategy. *IEEE Transactions on Evolutionary Computation*, volume 8, pages 149–172.

K. Deb, L. Thiele, M. L. and Zitzler, E. (2005). Scalable test problems for evolutionary multiobjective optimization. *IEEE Transactions on Evolutionary Computation*, volume 20, pages 105–145. Springer.

K. Deb, A. Samir, P. A. and Meyarivan, T. (2000). A fast elitist non-dominated sorting genetic algorithm for multi-objective optimization: NSGA-II. *IEEE Transactions on Evolutionary Computation*, pages 849–858. Springer.

Li, M., Yang, S., and Liu, X. (2014). Shift-based density estimation for pareto-based algorithms in many-objective optimization. *IEEE Transactions on Evolutionary Computation*, volume 18, pages 348–365.

Margarita, R. and Coello, C. C. A. (2006). Multi-objective particle swarm optimizers: A survey of the state-of-the-art. *International journal of computational inteligence research*, volume 2, pages 287–308.

X. Cai, Z. F. and Zhang, Q. (2017). A conatrained decomposition approach with grids for evolutionary multiobjective optimization. *IEEE Transactions on Evolutionary Computation*, volume 22, pages 564–557.

Yang, Shengxiang, L. M., Xiaohui, L., and Jinhua, Z. (2013). A grid-based evolutionary algorithm for many-objective optimization. *IEEE Transactions on Evolutionary Computation*, volume 17, pages 721–736.

Z. Eckart, K. J. and Lothar, T. (2008). Quality assessment of pareto set approximations. *In Evolutionary Multiobjective Optimization*, volume 52, pages 373–404. Springer.

Zhang, Q. and Li, H. (2007). MOEA/D: A multiobjective evolutionary algorithm based on decomposition. In *IEEE Transactions on Evolutionary Computation*, volume 11, pages 712–731.